# Optical Absorption and Emission Properties of Fluoranthene, Benzo[k]fluoranthene, and Their Derivatives. A DFT Study

**ARTICLE** *in* THE JOURNAL OF PHYSICAL CHEMISTRY A · NOVEMBER 2011

Impact Factor: 2.69 · DOI: 10.1021/jp208617s · Source: PubMed



**3 AUTHORS**, INCLUDING:

Saranya Govindarajan
Beijing Computational Science Research Ce…
**7** PUBLICATIONS **48** CITATIONS

SEE PROFILE

K. Senthilkumar
Bharathiar University
**77** PUBLICATIONS **1,443** CITATIONS

SEE PROFILE

THE JOURNAL OF PHYSICAL CHEMISTRY A

ARTICLE

pubs.acs.org/JPCA

# Optical Absorption and Emission Properties of Fluoranthene, Benzo[*k*]fluoranthene, and Their Derivatives. A DFT Study

G. Saranya, P. Kolandaivel, and K. Senthilkumar*

Department of Physics, Bharathiar University, Coimbatore, India-641 046

Supporting Information

**ABSTRACT:** Fluoranthene and benzo[*k*]fluoranthene-based oligoarenes are good candidates for organic light-emitting diodes (OLEDs). In this work, the electronic structure and optical properties of fluoranthene, benzo-[*k*]fluoranthene, and their derivatives have been studied using quantum chemical methods. The ground-state structures were optimized using the density functional theory (DFT) methods. The lowest singlet excited state was optimized using time-dependent density functional theory (TD-B3LYP) and configuration interaction singles (CIS) methods. On the basis of ground- and excited-state geometries, the absorption and emission spectra have been calculated using the TD-DFT method with a variety of exchange-correlation functionals. All the calculations were carried out in chloroform medium. The results show that the absorption and emission spectra calculated using the B3LYP functional is in good agreement with the available experimental results. Unlikely, the meta hybrid functionals such as M06HF and M062X underestimate the absorption and emission spectra of all the studied molecules. The calculated absorption and emission wavelength are more or less basis set independent. It has been observed that the substitution of an aromatic ring significantly alters the absorption and emission spectra.

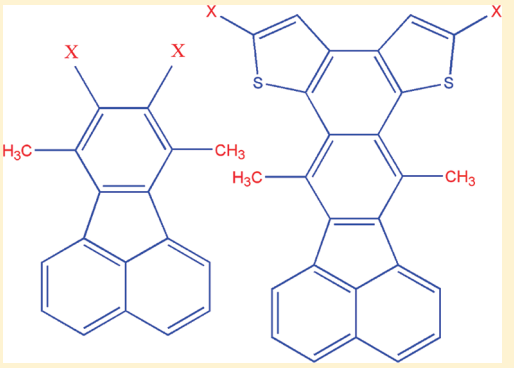


## 1. INTRODUCTION

Organic semiconductors[1,2] offer an alternative to inorganic semiconductors for applications in optoelectronic devices, such as field-effect transistors (FETs),[3−5] light-emitting diodes (LEDs),[6−8] solar cells,[9] photovoltaics, and nanoscale molecular electronic devices.[10] In comparison with inorganic semiconducting materials such as silicon, organic semiconductors can be easily processed with low-cost and low-temperature-processing techniques, such as spin-coating and inkjet printing,[11−13] which enable large area fabrication on a flexible substrate. Moreover, it is possible to tune their optoelectronic properties through chemical engineering. Among the several organic semiconducting materials, $\pi$-conjugated polycyclic aromatic hydrocarbons (PAHs) have attracted intense attention in the area of optoelectronics due to their unique properties of high thermal and air stability and excellent fluorescent emission.[14] To date, numerous PAHs such as anthracene, fluorene, pyrene, perylene, and fluoranthene have been extensively investigated for their potential application such as fluorescent sensors, organic nonlinear optical materials (NLO), and electroluminescent emitters (EL).[15−21]

A new family of PAHs, fluoranthene and benzo[*k*]fluoranthene-based novel heterooligoarenes, serve as a basic skeleton to prepare blue-light-emitting organic light-emitting diodes (OLEDs)[22−26] and organic field effect transistors (OFETs). Additionally, recent reports on fluoranthene scaffold include fabrication of highly efficient green OLEDs[27,28] and fluoranthene-based matrix material[29] with improved charge-carrier mobility. Recently, Yan et al.[22] synthesized fluoranthene derivatives through the Diels−Alder reaction between cyclopentadienone and 2,2′-(ethyne-1,2-diyl)-bisthiophene followed by decarbonylation. The bromination and subsequent substitution through a Suzuki coupling reaction and $FeCl_3$-mediated oxidative cyclization led to the formation of sulfur-heterobenzo[*k*]fluoranthene derivatives. These compounds exhibit good thermal and oxidative stability in air. Yan et al.[22] investigated the absorption and emission spectra of these compounds in chloroform solution and reported more than one absorption band and emission spectrum. Their results show that the absorption and emission spectra are in the UV-to-visible region and benzo[*k*]fluoranthene derivatives have liquid crystalline behavior.

To understand the experimentally observed optical properties of these compounds, theoretical investigations on the structure−property relationship of these materials are essential. Quantum chemical calculations are vital tools to investigate the relationship between electronic structures and the optical properties of the organic molecules. The aim of the present work is to investigate the ground- and excited-state geometries and the optical absorption and emission properties of fluoranthene, benzo[*k*]fluoranthene, and their substituted derivatives using various quantum chemical methods. The structures of the studied molecules, fluoranthene and benzo[*k*]fluoranthene, are shown in Figure 1.

The optimization of excited-state geometry is much more challenging than the optimization of ground-state geometry.

**Received:** September 7, 2011
**Revised:** November 11, 2011
**Published:** November 11, 2011

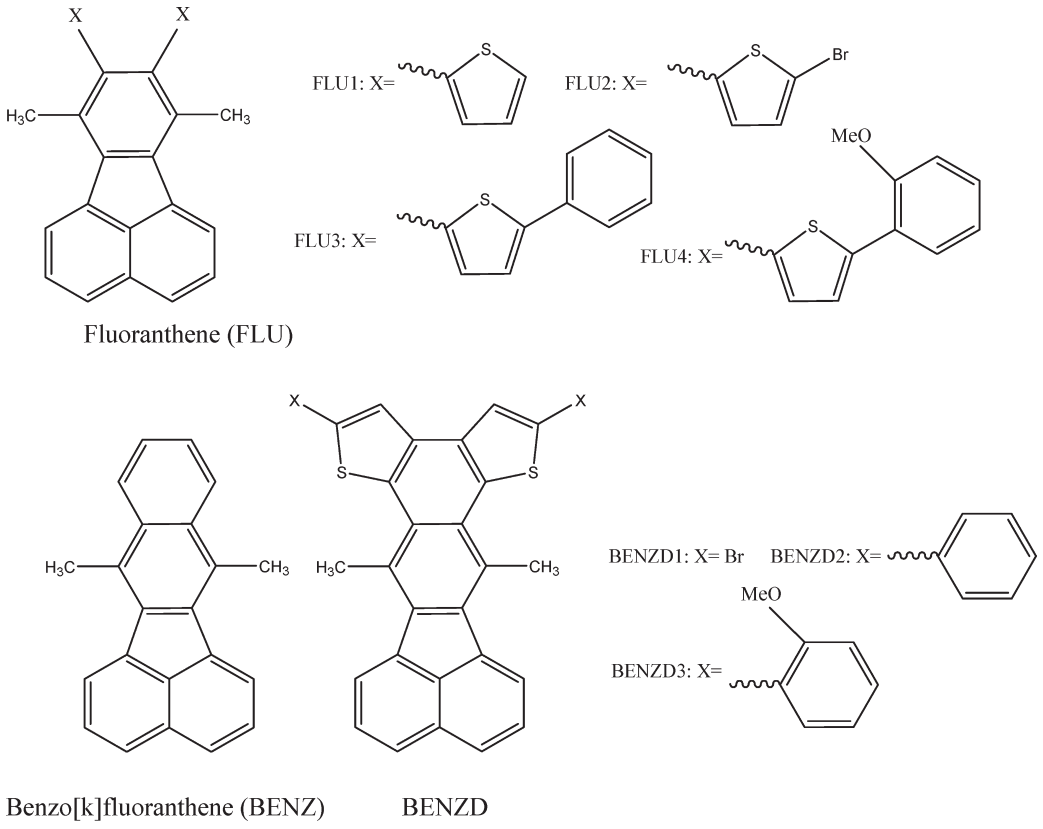


**Figure 1.** Chemical structure of fluoranthene, benzo[*k*]fluoranthene, and their derivatives.

This is because the excited states lack the analytical derivatives of the energy with respect to atomic displacements: that is, forces on atoms cannot be calculated directly. In addition, the information that can be extracted from experiment about the excited-state geometry is very limited. The wave function-based electron correlation methods such as CIS, CASPT2, SAC-CI, and MP2 are the best choices to calculate the excited-state geometry and optoelectronic properties. A quite good number of studies[30−33] reported the results obtained from the above highly sophisticated methods and found that in all the cases the results are comparable with the experimental results. However, these wave function-based electron correlated methods are highly expensive and can be applied to the molecules having very few atoms.

In recent years, time-dependent density functional theory (TD-DFT) has emerged as a reliable standard tool to study the absorption and emission spectra of organic molecules with few tenths of atoms, and recent reports demonstrate the good accuracy for a wide range of systems.[34−36] The computational cost of the TD-DFT calculation is less compared to that of wave function-based electron correlation methods. However, the accuracy of the TD-DFT depends on the so-called adiabatic approximation,[37,38] and the approximate ground-state exchange-correlation functional used in the DFT calculations.[39−43] Zhao et al.[44] used HF and CIS methods to optimize the ground- and excited-state geometries of coumarin 6 isomers. On the basis of these geometries, they calculated the absorption and emission spectra using the TD-DFT method with the B3LYP exchange-correlation functional, and their results are in good agreement with the experimental results. It has been shown in earlier studies that the results obtained with TD-B3LYP and CIS methods are in good agreement with the available experimental results for phenylene ethynylene oligomers,[45] luciferin,[46] and triphenylene derivatives.[47] Xue et al.[48,49] have shown that TD-DFT at PBE1PBE/6-31G//PBE1PBE/6-31G(d) level of theory successfully reproduced the molecular geometry and absorption wavelength of chalcones. However, few studies have shown that the TD-DFT methods underestimate the excitation energies of larger $\pi$-conjugated organic molecules.[50−53] Recently, new meta hybrid exchange-correlation functionals such as M062X and M06HF were developed to get highly accurate excitation energies. Y. Zhao and D. G. Truhlar[51] calculated the excitation energies for $N_2$, CO, HCHO, tetracene, $NH_3\cdots F_2$, and $C_2H_4\cdots C_2F_4$ using a variety of exchange-correlation functionals including meta hybrid functionals M062X and M06HF and concluded that the excitation energy value calculated from M06 functionals agrees well with the experimental values, whereas the other generalized gradient approximation (GGA)-based exchange-correlation functionals underestimate the excitation energy values. It has also been reported that M06HF is the best functional for the study of long-range charge transfer.[51] Recently Jacquemin et al.[52] reported that the M062X method provides better results than that of B3LYP and PBE1PBE methods for singlet−triplet transitions. In the present work, to identify the most appropriate method for the calculation of absorption and emission spectra of fluoranthene, benzo[*k*]fluoranthene, and their derivatives, we have employed the TD-DFT method with different exchange-correlation functionals and also the CIS method.

The organization of the paper is as follows. The computation details are given in section 2. Along with the benchmark studies, the optoelectronic properties of fluoranthene, benzo[*k*]fluoranthene, and their derivatives are discussed in section 3. Finally, the main conclusions are summarized in section 4.

## 2. COMPUTATIONAL DETAILS

To optimize the ground-state geometry of fluoranthene, benzo[*k*]-fluoranthene, and their derivatives, we have employed the B3LYP[40,41,54] and PBE1PBE[55−58] functionals in conjunction with the 6-311G(d,p) basis set. The B3LYP functional uses Becke's three-parameter exchange functional (B3)[41] together with the nonlocal correlation function provided by Lee−Yang−Parr (LYP)[54] and the local correlation functional of Vosko−Wilk−Nusair (VWN).[40] The PBE functional of Perdew−Burke−Ernzerhof[55,56] was made into a hybrid functional by Adamo[57] as PBE1PBE which includes 25% exchange and 75% correlation. All stationary points were conformed as energy minima in the potential energy surface using vibrational frequency calculations. The excited-state geometry of fluoranthene, benzo[*k*]fluoranthene, and their derivatives were optimized at TD-B3LYP/6-311G(d,p) and CIS/6-311G(d,p) level of theories. With the optimized ground- and excited-state geometries, the absorption and emission spectrum of fluoranthene, benzo[*k*]fluoranthene, and their derivatives were calculated using the TD-DFT method with B3LYP, PBE1PBE, M062X,[51] and M06HF[59] functionals and the 6-311G(d,p) basis set. The M062X and M06HF functionals include 54% and 100% of Hartree−Fock exchange, respectively.

The basis set dependence of absorption and emission spectra were studied for fluoranthene, benzo[*k*]fluoranthene, and their derivatives using TD-B3LYP functional. The basis sets comparison includes 6-31G(d), 6-31+G(d), 6-311G(d,p), and 6-311+G(d,p). The ground- and excited-state optimization and spectral calculations were carried out in chloroform medium using Tomasi's[60] polarized continuum model (PCM) in self-consistent reaction field (SCRF) theory to compare with the available experimental results. In the PCM method, the solute molecule is lying inside a cavity representing a solvent medium defined in terms of structureless material characterized by its dielectric constant, radius, density, and molecular volume. In the present study the dielectric constant of 4.71 is used to represent the chloroform medium. It has been shown in an earlier study that the substitution of methoxy group at the ortho, para, and meta positions of the phenyl ring in fluoranthene and benzo[*k*]fluoranthene derivatives gave nearly the same absorption and emission spectra.[22] Therefore, we have studied fluoranthene and benzo[*k*]fluoranthene derivatives with methoxy substitution at the ortho position of the phenyl ring only. Also, to reduce the computational expenses, the side chains $C_5H_{11}$ of fluoranthene, benzo[*k*]fluoranthene, and their derivatives were replaced by $CH_3$. It has been shown in earlier studies[61,62] that the effect of side chains on optical properties is negligible. All the calculations were performed using the Gaussian 09 program.[63]

## 3. RESULTS AND DISCUSSION

**Absorption Properties of Fluoranthene, Benzo[*k*]-fluoranthene, and Their Derivatives.** The ground-state geometry of fluoranthene, benzo[*k*]fluoranthene, and their derivatives has been optimized at B3LYP/6-311G(d,p) and PBE1PBE/6-311G(d,p) level of theories. Previous investigations on fluoranthene derivatives[64−68] reveal that the singlet ground state of these molecules exhibit diradical character. Hence, in the present work, the stability of diradical has been investigated for (methoxyphenyl)thiophene-substituted fluoranthene derivative (FLU4) and methoxyphenyl-substituted benzo[*k*]fluoranthene derivative (BENZ3), which have a minimum HOMO−LUMO gap among the studied derivatives. The calculations were carried out using a symmetry-broken UB3LYP/6-311G(d,p) level of theory. In comparison with the neutral system, the diradical configuration

**Table 1. Available Experimental Values and Computed Absorption Energies ($\lambda$ in nm and in eV) and Oscillator Strengths ($f$ in a.u.) of Fluoranthene and Its Derivatives with the TD-B3LYP//B3LYP Method Using the 6-311G(d,p) Basis Set in Chloroform Medium[a]**

| | | absorption energy ($\lambda$) | | | |
|---|---|---|---|---|---|
| system | expt[b](in nm) | in nm | in eV | transition | $f$ |
| FLU | | 366 | 3.38 | H-1→L | 0.06 |
| | 360 | 349 | 3.55 | H→L | 0.25 |
| | 344 | 297 | 4.17 | H-2→L | 0.05 |
| | 324 | 269 | 4.62 | H-1→L+1 | 0.22 |
| | 289 | 258 | 4.81 | H→L+1 | 0.06 |
| | | 254 | 4.89 | H-3→L | 0.22 |
| | | 235 | 5.27 | H-1→L+2 | 0.14 |
| | | 221 | 5.6 | H-2→L+1 | 0.15 |
| | | 215 | 5.75 | H-4→L | 0.02 |
| FLU1 | | 380 | 3.26 | H-1→L | 0.03 |
| | 383 | 365 | 3.39 | H→L | 0.41 |
| | 366 | 299 | 4.15 | H-5→L | 0.06 |
| | 287 | 284 | 4.36 | H-7→L | 0.1 |
| | 274 | 268 | 4.62 | H-1→L+1 | 0.43 |
| | | 264 | 4.7 | H→L+1 | 0.02 |
| FLU2 | – | 380 | 3.27 | H-1→L | 0.04 |
| | | 366 | 3.38 | H→L | 0.45 |
| | | 300 | 4.14 | H-4→L | 0.07 |
| | | 287 | 4.32 | H-5→L | 0.06 |
| | | 284 | 4.36 | H-6→L | 0.09 |
| | | 276 | 4.49 | H→L+1 | 0.11 |
| | | 274 | 4.51 | H→L+2 | 0.16 |
| | | 272 | 4.56 | H-1→L+1 | 0.09 |
| FLU3 | | 403 | 3.08 | H→L | 0.07 |
| | | 372 | 3.33 | H-1→L | 0.3 |
| | 384 | 367 | 3.38 | H-3→L | 0.13 |
| | 364 | 353 | 3.51 | H-2→L | 0.1 |
| | 299 | 319 | 3.88 | H→L+1 | 0.25 |
| | | 305 | 4.06 | H→L+2 | 0.32 |
| | | 299 | 4.15 | H-5→L | 0.06 |
| | | 298 | 4.16 | H-4→L | 0.04 |
| | | 296 | 4.19 | H-1→L+1 | 0.51 |
| | | 289 | 4.29 | H-2→L+1 | 0.14 |
| FLU4 | | 416 | 2.98 | H→L | 0.04 |
| | | 393 | 3.15 | H-1→L | 0.39 |
| | 384 | 370 | 3.35 | H-3→L | 0.08 |
| | 369 | 363 | 3.42 | H-2→L | 0.42 |
| | 313 | 334 | 3.71 | H→L+1 | 0.25 |
| | 298 | 318 | 3.9 | H→L+2 | 0.23 |
| | | 310 | 4 | H-1→L+1 | 0.66 |
| | | 309 | 4.01 | H-4→L | 0.04 |
| | | 303 | 4.09 | H-5→L | 0.01 |
| | | 299 | 4.1 | H-1→L+2 | 0.13 |

[a] The transitions with oscillator strength higher than 0.01 a.u. are given. [b] Taken from ref 22.

**Table 2. Available Experimental Values and the Computed Absorption Energies ($\lambda$ in nm and in eV) and Oscillator Strengths ($f$ in a.u.) of Benzo[$k$]fluoranthene and Its Derivatives with the TD-B3LYP//B3LYP Method Using the 6-311G (d,p) Basis Set in Chloroform Medium[a]**

| | | absorption energy ($\lambda$) | | | |
|---|---|---|---|---|---|
| system | expt[b](in nm) | in nm | in eV | transition | $f$ |
| BENZ | – | 387 | 3.2 | H→L | 0.35 |
| | | 332 | 3.73 | H→L+1 | 0.01 |
| | | 297 | 4.17 | H-1→L+1 | 0.61 |
| | | 282 | 4.4 | H-2→L | 0.45 |
| | | 256 | 4.84 | H-3→L+1 | 0.03 |
| | | 251 | 4.95 | H→L+2 | 0.45 |
| | | 243 | 5.1 | H-1→L+2 | 0.2 |
| BENZD1 | | 419 | 2.96 | H→L | 0.45 |
| | 436 | 396 | 3.13 | H-1→L | 0.06 |
| | 411 | 349 | 3.55 | H→L+1 | 0.02 |
| | 390 | 337 | 3.68 | H-1→L+1 | 0.97 |
| | 341 | 308 | 4.02 | H-3→L | 0.07 |
| | 302 | 299 | 4.15 | H→L+2 | 0.35 |
| | 289 | 289 | 4.29 | H-1→L+2 | 0.16 |
| | | 284 | 4.37 | H-4→L | 0.1 |
| BENZD2 | | 441 | 2.81 | H→L | 0.57 |
| | 450 | 422 | 2.94 | H-1→L | 0.21 |
| | 424 | 359 | 3.45 | H-1→L+1 | 1.07 |
| | 355 | 340 | 3.65 | H→L+2 | 0.22 |
| | 340 | 337 | 3.68 | H-1→L+2 | 0.45 |
| | | 327 | 3.79 | H-2→L | 0.02 |
| | | 315 | 3.93 | H-4→L | 0.04 |
| | | 308 | 4.02 | H-3→L | 0.09 |
| | | 304 | 4.08 | H→L+3 | 0.08 |
| BENZD3 | | 450 | 2.76 | H→L | 0.58 |
| | 455 | 438 | 2.83 | H-1→L | 0.23 |
| | 429 | 366 | 3.39 | H-1→L+1 | 0.93 |
| | 360 | 365 | 3.4 | H→L+1 | 0.08 |
| | 343 | 347 | 3.58 | H-1→L+2 | 0.47 |
| | | 344 | 3.6 | H→L+2 | 0.22 |
| | | 331 | 3.75 | H-2→L | 0.02 |
| | | 311 | 3.99 | H→L+3 | 0.14 |

[a] The transitions with oscillator strength higher than 0.01 a.u. are given. [b] Taken from ref 22.

is less stable by 2.10 eV for FLU4 and 2.18 eV for BENZ3. Hence, further studies are carried out for the neutral system. The structural parameters obtained with B3LYP and PBE1PBE methods are very similar. The average root-mean-square deviation (rmsd) between the internal coordinates obtained from the B3LYP and PBE1PBE methods is 0.09 Å. Previous DFT studies on the absorption and emission spectra of chalcones[69] show that the ground-state geometry obtained from B3LYP and PBE1PBE methods are nearly same. The absorption characteristics of fluoranthene, benzo[$k$]fluoranthene, and their derivatives calculated with B3LYP//B3LYP, PBE1PBE//B3LYP, and PBE1PBE//PBE1PBE methods using the 6-311G(d,p) basis set together with experimental values of Yan et al.[22] are summarized in Tables 1 and 2, and Tables S1 and S2 (Supporting Information). To study the nature and energy of the singlet−singlet electronic

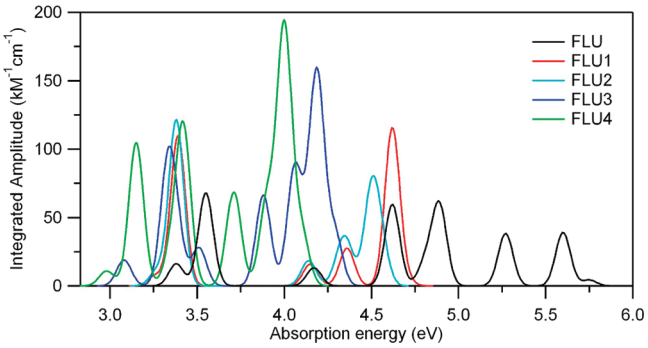


**Figure 2.** The absorption spectra of fluoranthene and its derivatives computed at TD-B3LYP/6−11G(d,p) level of theory in chloroform medium. (The spectra were simulated by using a Gaussian distribution centered at the computed absorption energies with an arbitrary width of 0.05 eV and an integrated amplitude equal to the calculated oscillator strengths).

transition and to compare with the available experimental values, the first 10 low-lying excited-state transitions have been calculated. From Tables 1 and 2, and Tables S1 and S2, it has been observed that for all the studied molecules, the absorption spectra calculated with the B3LYP//B3LYP method in chloroform medium agrees well with the experimental values. The PBE1PBE//B3LYP and PBE1PBE//PBE1PBE methods underestimate the absorption spectrum by 0.04 to 0.12 eV for all the molecules compared with experimental and B3LYP//B3LYP results (see Tables S1 and S2). Further, the orbital transitions corresponding to noted absorption bands are similar in these three methods (see Tables 1 and 2, Tables S1 and S2). The calculated absorption spectra using meta hybrid functionals TD-M062X and TD-M06HF with the 6-311G(d,p) basis set are summarized in Tables S3 and S4 (Supporting Information). In comparison with the available experimental and theoretical results, TD-M062X and TD-M06HF functionals underestimate the absorption spectra about 0.33 to 0.55 eV and 0.68 to 0.90 eV, respectively. In Tables S5 and S6 (Supporting Information), we have summarized the calculated absorption wavelength of fluoranthene, benzo[$k$]fluoranthene, and their derivatives using different basis sets with the B3LYP functional. It has been observed that the absorption wavelength calculated using 6-31G(d), 6-31+G(d), 6-311G(d,p) and 6-311+G(d,p) basis sets are nearly similar and the maximum variation is only around 0.06 eV. Particularly, the absorption features obtained from 6-31+G(d) and 6-311G(d,p) basis sets are similar. From the above discussion, we concluded that the effect of the basis set on the absorption spectrum of fluoranthene, benzo[$k$]fluoranthene, and their derivatives is negligible. Since the absorption wavelength calculated with the B3LYP//B3LYP method using the 6-311G(d,p) basis set is in better agreement with the experimental values, the results obtained with the B3LYP//B3LYP method is discussed in detail.

The calculated absorption energies for fluoranthene and its derivatives, thiophene (FLU1)-, bromothiophene (FLU2)-, phenylthiophene (FLU3)-, and (methoxyphenyl)thiophene (FLU4)-substituted fluoranthene at TD-B3LYP/6-311G(d,p) level of theory in chloroform medium, were plotted with respect to integrated amplitude and is shown in Figure 2. It has been observed that the absorption spectrum of fluoranthene exhibits three major bands, and the dominant absorption band is observed at 3.55 eV (349 nm), which is associated with the H→L transition.

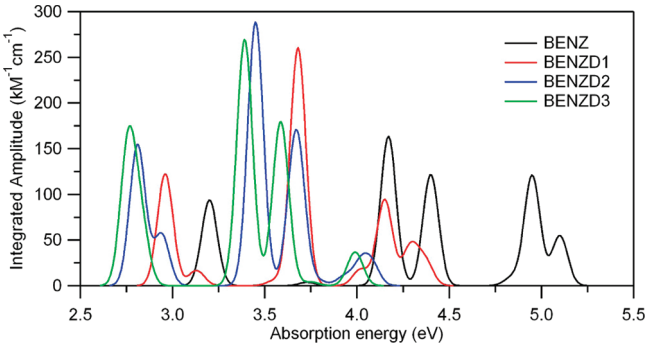


**Figure 3.** The absorption spectra of benzo[*k*]fluoranthene and its derivatives computed at TD-B3LYP/6−11G(d,p) level of theory in chloroform medium. (The spectra were simulated by using a Gaussian distribution centered at the computed absorption energies with an arbitrary width of 0.05 eV and an integrated amplitude equal to the calculated oscillator strengths).

The second and third intense bands are observed around 4.62 eV (269 nm) and 4.89 eV (254 nm), respectively, which are associated with H-1→L+1 and H-3→L transitions.

As shown in Figure 2, the absorption maxima ($\lambda_{max}$) of FLU1 and FLU2 exhibit a red-shift of about 15 nm compared with the $\lambda_{max}$ of fluoranthene, due to the substitution of thiophene and bromothiophene rings, whereas FLU3 and FLU4 exhibit a red-shift of about 40 and 50 nm, respectively, due to the substitution of phenylthiophene and (methoxyphenyl)thiophene rings. The absorption spectrum of FLU1 exhibits two major bands; the dominant absorption band observed at 4.62 eV (268 nm) is associated with the H-1→L+1 transition, and the second dominant band observed at 3.39 eV (365 nm) is due to the H→L transition. The absorption spectrum of FLU2 exhibits single band at 3.38 eV (366 nm) which corresponds to the H→L transition. The absorption spectrum of phenylthiophene-substituted fluoranthene (FLU3) exhibits three major bands, and the dominant absorption band is observed at 4.19 eV (296 nm), which is associated with the H-1→L+1 transition. The second and third intense bands are observed around 4.05 eV (305 nm) and 3.33 eV (372 nm), respectively, and are associated with the H→L+2 and H-1→L transitions. (Methoxyphenyl)thiophene-substituted fluoranthene (FLU4) also has three major absorption bands, and the dominant absorption band is observed at 4 eV (310 nm), which is associated with the H-1→L+1 transition. The second and third intense bands are observed around 3.42 eV (363 nm) and 3.15 eV (393 nm), respectively, and are associated with H-2→L and H-1→L transitions. That is, the substitution with an electron-donating group on fluoranthene increases the absorption wavelength.

For benzo[*k*]fluoranthene and bromine (BENZD1)-, phenyl (BENZD2)-, and methoxyphenyl (BENZD3)-substituted benzo[*k*]fluoranthene derivatives, the absorption energies calculated at TD-B3LYP/6-311G(d,p) level of theory in chloroform medium were plotted with respect to integrated amplitude and is shown in Figure 3. As shown in Figure 3, the absorption maxima ($\lambda_{max}$) of benzo[*k*]fluoranthene has been noted at 3.20 eV (387 nm), which is associated with the H→L transition. Additionally three intense bands are observed at 4.17 eV (297 nm), 4.40 eV (282 nm), and 4.95 eV (251 nm) and are associated with the H-1→L, H-2→L and H→L+1 transitions, respectively. In comparison with benzo[*k*]fluoranthene, the $\lambda_{max}$ of bromine-substituted benzo[*k*]fluoranthene derivative (BENZD1) was red-shifted about 28 nm, and for phenyl- and methoxyphenyl-substituted benzo[*k*]fluoranthene derivatives (BENZD2 and BENZD3), the red-shift is about 54 and 63 nm, respectively, owing to the increase of effective conjugation length with the introduction of aromatic substitutions. As shown in Figure 3, the absorption spectrum of BENZD1 exhibits three major bands, and the dominant absorption band is observed at 3.68 eV (337 nm), which is associated with the H-1→L+1 transition. The second and third intense bands are observed around 2.96 eV (419 nm) and 4.15 eV (299 nm), respectively, and the corresponding transitions are H→L and H→L+2. The absorption spectrum of BENZD2 exhibits three major bands, and the dominant absorption band is observed at 3.45 eV (359 nm), which is associated with the H-1→L+1 transition. The second and third intense bands are observed around 2.81 eV (441 nm) and 3.68 eV (337 nm), respectively, and are associated with the H→L and H-1→L+2 transitions. As observed in BENZD2, the absorption spectrum of BENZD3 also exhibits three major bands, but they are red-shifted about 7−10 nm with the same orbital transitions. In comparison with the absorption spectrum of fluoranthene and its derivatives, the absorption spectrum of benzo[*k*]fluoranthene and its derivatives are red-shifted about 20 to 35 nm, which is in agreement with the available experimental results.[22] This red-shift is mainly due to the formation of larger polycyclic aromatic skeleton.

**Table 3. Ground-State Dipole Moment (in Debye) of Fluoranthene, Benzo[*k*]fluoranthene, and Their Derivatives Calculated at B3LYP and PBE1PBE Methods Using the 6-311G(d,p) Basis Set in Chloroform Medium**

| system | B3LYP | PBE1PBE |
|---|---|---|
| FLU | 0.45 | 0.44 |
| FLU 1 | 1.59 | 1.41 |
| FLU 2 | 5.03 | 4.65 |
| FLU 3 | 1.42 | 1.34 |
| FLU 4 | 3.01 | 2.94 |
| BENZ | 0.39 | 0.38 |
| BENZD1 | 2.31 | 2.22 |
| BENZD2 | 0.98 | 0.95 |
| BENZD3 | 1.33 | 1.23 |

**Dipole Moment.** The dipole moment of the fluoranthene, benzo[*k*]fluoranthene, and their derivatives in chloroform medium is summarized in Table 3. It has been observed that the dipole moment calculated at B3LYP/6-311G(d,p) and PBE1PBE/6-311G(d,p) level of theories are similar. The dipole moment value of fluoranthene is 0.45 D and benzo[*k*]fluoranthene is 0.39 D at B3LYP/6-311G(d,p) level of theory. It has been observed that the substitution increases the dipole moment value and the effect is significant in fluoranthene. The bromothiophene-substituted fluoranthene (FLU2) and benzo[*k*]fluoranthene derivatives (BENZD1) have relatively larger dipole moment value of 5.03 and 2.31 D, respectively.

**Molecular Orbital Energies.** Energy levels of the frontier molecular orbitals especially HOMO and LUMO as well as their spatial distributions are crucial parameters for determining the optoelectronic properties. The density plot of the HOMO and LUMO of fluoranthene, benzo[*k*]fluoranthene, and their derivatives are calculated at B3LYP/6-311G(d,p) level of theory and are shown in Figures 4 and 5, respectively. The orbital diagrams

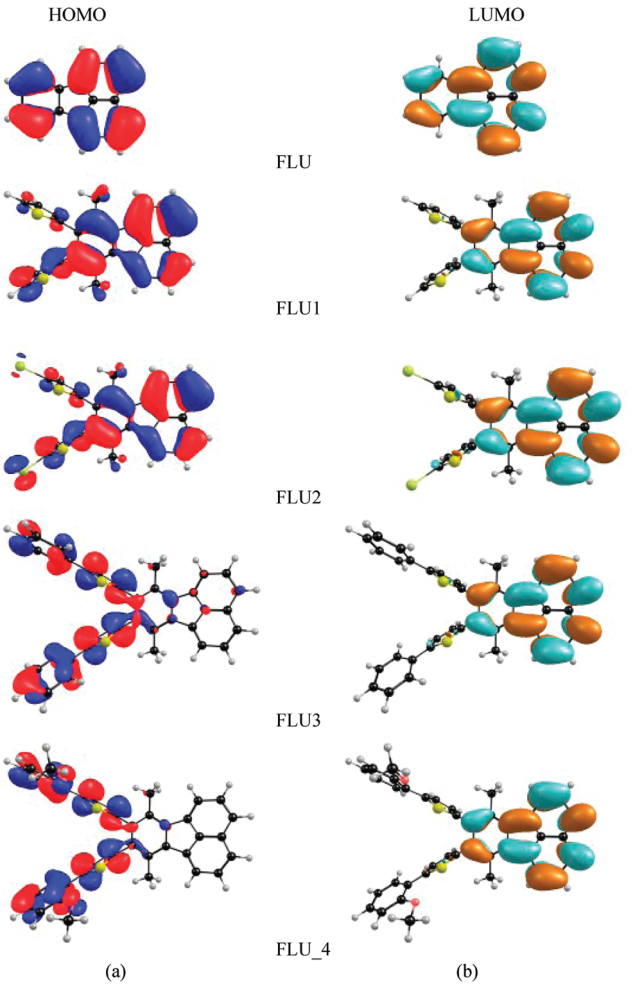


**Figure 4.** The density plot of (a) the highest occupied molecular orbital (HOMO) and (b) the lowest unoccupied molecular orbital (LUMO) of fluoranthene and its derivatives calculated at B3LYP/6-311G(d,p) level of theory in chloroform medium.

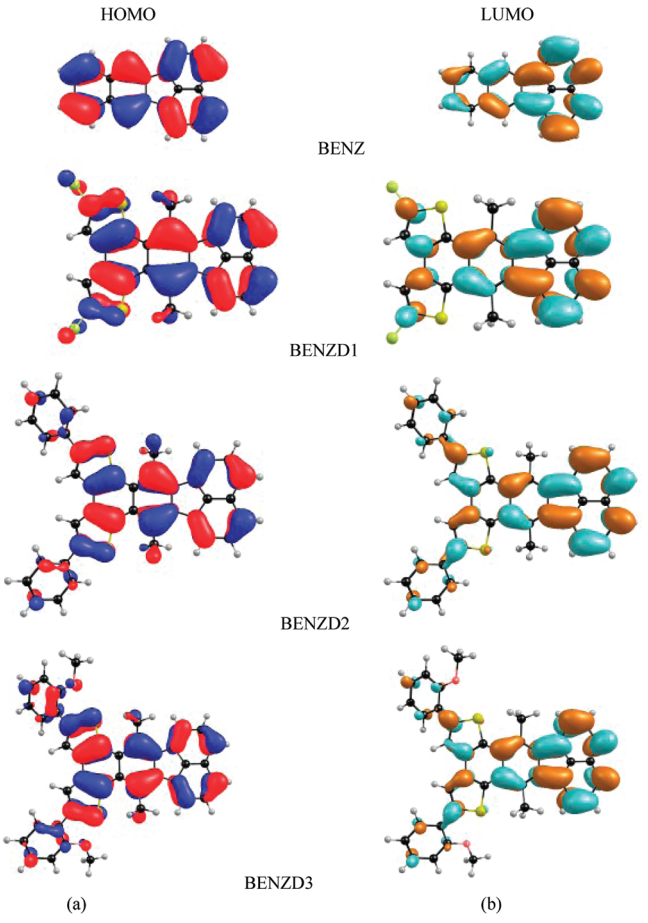


**Figure 5.** The density plot of (a) the highest occupied molecular orbital (HOMO) and (b) the lowest unoccupied molecular orbital (LUMO) of benzo[*k*]fluoranthene and its derivatives calculated at B3LYP/6-311G(d,p) level of theory in chloroform medium.

are plotted with the contour value of 0.025 a.u. The plots of the HOMO and LUMO of the studied molecules have the typical $\pi$ molecular orbital characteristics and are slightly altered by the substitution. From the molecular orbital analysis, we infer that the lowest lying singlet−singlet absorption as well as emission corresponds to the electronic transition of $\pi \rightarrow \pi^*$ type. Figure 4 illustrates that, for fluoranthene, both HOMO and LUMO are fully delocalized over the entire molecular system. The introduction of thiophene (FLU1) and bromothiophene (FLU2) to fluoranthene slightly alters the HOMO, and LUMO is delocalized only on the fluoranthene core. For both FLU3 and FLU4, the HOMO is delocalized on the aromatic substitutions, whereas LUMO is delocalized on the fluoranthene core. As observed for fluoranthene, the HOMO and LUMO of benzo[*k*]fluoranthene are fully delocalized over the entire molecular system (see Figure 5).

The energy of the frontier molecular orbitals of fluoranthene, benzo[*k*]fluoranthene, and their derivatives obtained at B3LYP/6-311G(d,p) level of theory are presented in Figures 6 and 7. The HOMO (H)−LUMO (L) energy gap of fluoranthene and benzo[*k*]fluoranthene is 3.99 and 3.65 eV, respectively. For both fluoranthene and benzo[*k*]fluoranthene, the HOMO energy is slightly increased upon substitution. It has been observed that the

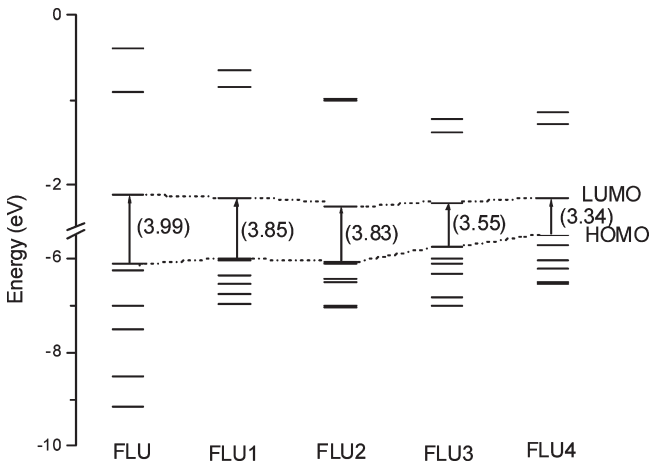


**Figure 6.** Energy level diagrams of frontier molecular orbitals of fluoranthene and its derivatives. Energy gap value (in eV) is given within parentheses.

H−L energy gap slightly decreased upon the substitution in fluoranthene and benzo[*k*]fluoranthene molecules. As expected, the molecules with a small H−L energy gap possess maximum absorption and emission wavelength. Among the fluoranthene

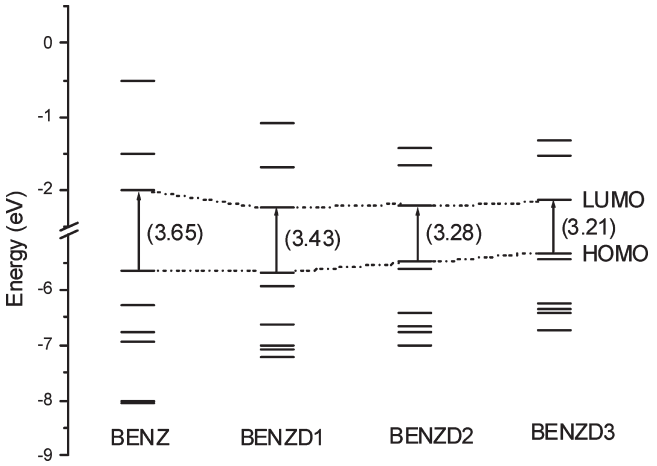


**Figure 7.** Energy level diagrams of frontier molecular orbitals of benzo[*k*]fluoranthene and its derivatives. Energy gap value (in eV) is given within parentheses.

derivatives, FLU4 has a minimum H−L energy gap of 3.34 eV and has a maximum absorption and emission wavelength of 416 nm (2.98 eV) and 545 nm (2.27 eV), respectively. Similarly, among benzo[*k*]fluoranthene derivatives, BENZD3 has a minimum H−L energy gap of 3.21 eV and a maximum absorption and emission wavelength of 450 nm (2.76 eV) and 522 nm (2.38 eV), respectively. Note that the H−L energy gap of the benzo[*k*]-fluoranthene is less than that of the fluoranthene by 0.34 eV. The above results show that the substitutions alter the spatial charge distribution and energy of the frontier molecular orbitals, and hence the spectral properties depend on the substitution groups.

**Emission Properties of Fluoranthene, Benzo[*k*]fluoranthene, and Their Derivatives.** The excited-state geometry of fluoranthene, benzo[*k*]fluoranthene, and their derivatives has been optimized by using the TD-B3LYP and singly excited configuration interaction (CIS) method with the 6-311G(d,p) basis set in chloroform medium. The structural parameters obtained with the TD-B3LYP and CIS methods are similar. The average root-mean-square deviation (rmsd) between the internal coordinates obtained from the TD-B3LYP and CIS methods is 0.5 Å. The emission spectra were obtained using the TD-DFT method at TD-B3LYP/6-311G(d,p) and TD-PBE1PBE/6-311G(d,p) level of theories. Along with the available experimental results, the calculated emission wavelength and corresponding oscillator strength for fluoranthene, benzo[*k*]fluoranthene, and their substituted derivatives are summarized in Table 4, and Table S7 (Supporting Information). It has been observed that the emission wavelength calculated through TD-B3LYP and TD-PBE1PBE methods based on the TD-B3LYP excited-state geometry is in good agreement with the experimental values, i.e., the average deviation is only about 0.09 eV. But the average deviation of the calculated emission wavelength with respect to the experimental values is about 0.13 eV with the TD-B3LYP//CIS and TD-PBE1PBE//CIS methods. From Tables 4 and S7, it has been observed that the emission spectra obtained from the TD-B3LYP and TD-PBE1PBE methods are similar. Further, the orbital transitions calculated from TD-B3LYP and TD-PBE1PBE methods are nearly the same with TD-B3LYP and CIS geometry. The calculated emission wavelength using meta hybrid functionals TD-M062X and TD-M06HF with the 6-311G(d,p) basis set based on TD-B3LYP/6-311G(d,p) excited-state geometry are

**Table 4. Available Experimental Values and the Computed Emission Energies ($\lambda$ in nm) and Oscillator Strengths ($f$ in a. u.) of Fluoranthene and Its Derivatives with the TD-B3LYP//TD-B3LYP Method Using the 6-311G(d,p) Basis Set in Chloroform Medium[a]**

| | | absorption energy ($\lambda$) | | | |
|---|---|---|---|---|---|
| system | expt[b](in nm) | in nm | in eV | $f$ | transition |
| FLU | 463 | 486 | 2.55 | 0.01 | H→L |
| | | 398 | 3.12 | 0.25 | H-1→L |
| | 443 | 311 | 3.98 | 0.08 | H-2→L |
| FLU1 | 467 | 498 | 2.49 | 0.04 | H→L |
| | | 425 | 2.92 | 0.44 | H-1→L |
| | | 381 | 3.26 | 0.01 | H-2→L |
| FLU2 | – | 508 | 2.44 | 0.06 | H→L |
| | | 427 | 2.9 | 0.49 | H-1→L |
| | | 386 | 3.21 | 0.01 | H-2→L |
| FLU3 | 500 | 533 | 2.33 | 0.12 | H→L |
| | | 452 | 2.74 | 0.59 | H-1→L |
| | | 401 | 3.1 | 0.07 | H-3→L |
| FLU4 | 513 | 545 | 2.27 | 0.1 | H→L |
| | | 467 | 2.66 | 0.49 | H-1→L |
| | | 407 | 3.05 | 0.03 | H-3→L |
| BENZ | - | 435 | 2.85 | 0.37 | H→L |
| | | 353 | 3.5 | 0.01 | H→L+1 |
| BENZD1 | 448 | 465 | 2.67 | 0.49 | H→L |
| | | 438 | 2.83 | 0.05 | H-1→L |
| | | 370 | 3.35 | 0.01 | H→L+1 |
| BENZD2 | 465 | 496 | 2.5 | 0.61 | H→L |
| | | 465 | 2.67 | 0.21 | H-1→L |
| | | 395 | 3.29 | 0.32 | H→L+1 |
| BENZD3 | 472 | 522 | 2.38 | 0.43 | H→L |
| | | 484 | 2.56 | 0.39 | H-1→L |
| | | 400 | 3.1 | 0.21 | H→L+1 |

[a] The transitions with oscillator strength higher than 0.01 a.u. are given. [b] Taken from ref 22.

summarized in Table S8 (Supporting Information). In comparison with the available experimental results and the results obtained from the TD-B3LYP and TD-PBE1PBE methods, it has been observed that TD-M062X and TD-M06HF functionals underestimate the emission spectra about 0.15−0.32 eV and 0.44−0.83 eV, respectively. In Table S9 (Supporting Information), we have summarized the calculated emission wavelength for fluoranthene, benzo[*k*]fluoranthene, and their derivatives using different basis sets with the B3LYP functional. It has been found that the emission wavelength calculated using 6-31G(d), 6-31+G(d), 6-311G(d,p), and 6-311+G(d,p) basis sets are nearly similar, and the maximum deviation is only about 0.06 eV. Particularly, as observed for absorption spectra, the emission features obtained with 6-31+G(d) and 6-311G(d,p) basis sets are similar. From the above discussions, we concluded that the effect of the basis set on the emission spectrum of fluoranthene, benzo[*k*]fluoranthene, and their derivatives is negligible. Therefore, as discussed for absorption spectra, the emission spectra is also discussed with the data obtained at the TD-B3LYP/6-311G(d,p) level of theory.

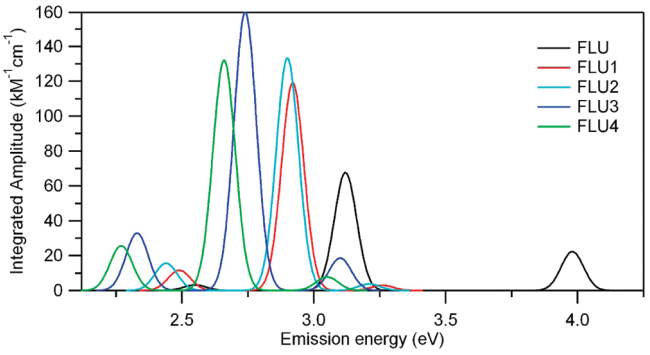


**Figure 8.** The emission spectra of fluoranthene and its derivatives computed at TD-B3LYP/6−11G(d,p) level of theory in chloroform medium. (The spectra were simulated by using a Gaussian distribution centered at the computed emission energies with an arbitrary width of 0.05 eV and an integrated amplitude equal to the calculated oscillator strengths).

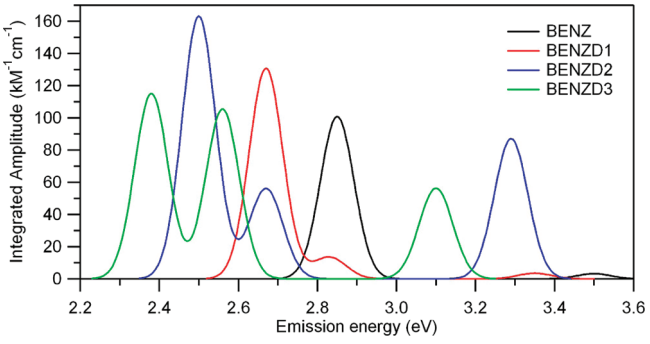


**Figure 9.** The emission spectra of benzo[*k*]fluoranthene and its derivatives computed at TD-B3LYP/6−11G(d,p) level of theory in chloroform medium. (The spectra were simulated by using a Gaussian distribution centered at the computed emission energies with an arbitrary width of 0.05 eV and an integrated amplitude equal to the calculated oscillator strengths).

For fluoranthene and its derivatives, the emission energies calculated at the TD-B3LYP/6-311G(d,p) level of theory in chloroform medium were plotted with respect to integrated amplitude and is shown in Figure 8. It has been observed that the emission maximum ($\lambda_{max}$) of fluoranthene was observed at 2.55 eV (486 nm), which is associated with the H→L transition. In comparison with the fluoranthene, the $\lambda_{max}$ of FLU1 and FLU2 is red-shifted about 10 and 20 nm, respectively, due to the substitution of thiophene and bromothiophene ring. Similarly, for FLU3 and FLU4, the emission spectra is red-shifted about 50 nm compared with the $\lambda_{max}$ of fluoranthene. As shown in Figure 8, the emission spectrum of fluoranthene and its derivatives exhibits three peaks, and the second peak has maximum intensity, which is associated with the H-1→L transition.

For benzo[*k*]fluoranthene and its derivatives, the emission energies calculated at TD-B3LYP/6-311G(d,p) level of theory in chloroform medium were plotted with respect to the integrated amplitude and is shown in Figure 9. The emission maximum ($\lambda_{max}$) of benzo[*k*]fluoranthene has been observed at 2.85 eV (435 nm), which is associated with the H→L transition. As observed for fluoranthene and its derivatives, the emission spectrum of benzo[*k*]fluoranthene derivatives is also red-shifted about 30−70 nm because of the substitutions. As shown in Figure 9, the dominant band is associated with the H→L transition. In comparison with the emission spectrum of fluoranthene and its derivatives, the emission spectrum of benzo[*k*]fluoranthene and its derivatives are blue-shifted about 20−50 nm. This blue-shift is due to the formation of a larger polycyclic aromatic skeleton.

## 4. CONCLUSION

The quantum chemical calculations were performed to investigate the optoelectronic properties of fluoranthene, benzo[*k*]fluoranthene, and their derivatives. The ground-state structure has been optimized at B3LYP/6-311G(d,p) and PBE1PBE/6-311G(d,p) level of theories. The lowest singlet excited-state geometry was optimized using time-dependent density functional theory (TD-DFT) and configuration interaction singles (CIS) methods with the 6-311G(d,p) basis set. The absorption and emission spectra have been calculated using the TD-DFT method with B3LYP, PBE1PBE, and meta hybrid functionals, M062X and M06HF, based on ground- and excited-state geometries. All the calculations were carried out in chloroform medium by using the polarizable continuum model (PCM). It has been observed that the effect of the basis set on the calculated absorption and emission spectra of these molecules is negligible. The results show that the calculated absorption and emission spectra using the B3LYP method is in good agreement with the experimental results. The meta hybrid functionals TD-M06HF and TD-M062X underestimate the absorption and emission spectra of all the studied molecules. It has been observed that the dipole moment of fluoranthene and benzo[*k*]fluoranthene increases and the HOMO−LUMO (H−L) energy gap is decreased by the substitution on the fluoranthene and benzo[*k*]-fluoranthene core. The substitution of aromatic rings significantly affects the absorption and emission spectra. Among the fluoranthene derivatives, (methoxyphenyl)thiophene-substituted fluoranthene has a minimum H−L energy gap of 3.34 eV and has a maximum absorption and emission wavelength of 416 nm (2.98 eV) and 545 nm (2.27 eV), respectively. Similarly, for benzo[*k*]fluoranthene derivatives, the methoxyphenyl-substituted benzo[*k*]fluoranthene derivative has minimum H−L energy gap of 3.21 eV and has a maximum absorption and emission wavelength of 450 nm (2.76 eV) and 522 nm (2.38 eV), respectively. The results obtained from this theoretical investigation confirm that the optical properties of fluoranthene and benzo[*k*]fluoranthene are significantly tuned by suitable substitution and that these compounds can be used as a basic skeleton to prepare efficient organic LEDs.

## ■ ASSOCIATED CONTENT

**Ⓢ Supporting Information.** Absorption spectra calculated with TD-PBE1PBE//B3LYP, TD-PBE1PBE//PBE1PBE, TD-M062X//B3LYP, and TD-M06HF//B3LYP using the 6-311G(d,p) basis set for fluoranthene, benzo[*k*]fluoranthene, and their derivatives in chloroform medium are summarized in Tables S1−S4. Similarly, the emission spectra calculated with TD-PBE1PBE//TD-B3LYP, TD-B3LYP//CIS, TD-PBE1PBE//CIS, TD-M062X//TD-B3LYP, and TD-M06HF//TD-B3LYP using the 6-311G(d,p) basis set for the studied molecules are summarized in Tables S7 and S8. The absorption and emission spectra calculated at TD-B3LYP//B3LYP and TD-B3LYP//CIS with the basis sets 6-31G(d), 6-31+(d), 6-311G(d,p), and 6-311

+G(d,p) are summarized in Tables S5, S6, and S9. This material is available free of charge via the Internet at http://pubs.acs.org.

## AUTHOR INFORMATION

**Corresponding Author**
*Fax: +91-422-2422387. E-mail: ksenthil@buc.edu.in.

## ACKNOWLEDGMENT

K.S. thanks the Department of Science and Technology (DST), India, for granting a research project under the DST-Fast track scheme.

## REFERENCES

(1) Warman, J. M.; de Haas, M. P.; Dicker, G.; Grozema, F. C.; Piris, J.; Debije, M. *Chem. Mater.* **2004**, *16*, 4600–4609.
(2) Anthony, J. E. *Chem. Rev.* **2006**, *106*, 5028–5048.
(3) Bao, Z.; Lovinger, A. J.; Brown, J. *J. Am. Chem. Soc.* **1998**, *120*, 207–208.
(4) Newman, C. R.; Frisbie, C. D.; da Silva Filho, D. A.; Bredas, J. L.; Ewbank, P. C.; Mann, K. R. *Chem. Mater.* **2004**, *16*, 4436–4451.
(5) van Breemen, A. J. J. M.; Herwig, P. T.; Chlon, C. H. T.; Sweelssen, J.; Schoo, H. F. M.; Setayesh, S.; Hardeman, W. M.; Martin, C. A.; de Leeuw, D. M.; Valeton, J. J. P.; et al. *J. Am. Chem. Soc.* **2006**, *128*, 2336–2345.
(6) Gao, Z. Q.; Li, Z. H.; Xia, P. F.; Wong, M. S.; Cheah, K. W.; Chen, C. H. *Adv. Funct. Mater.* **2007**, *17*, 3194–3199.
(7) Christ, T.; Glusen, B.; Greiner, A.; Kettner, A.; Sander, R.; Stumpflen, V.; Tsukruk, V.; Wendorff, J. H. *Adv. Mater.* **1997**, *9*, 48–52.
(8) Hassheider, T.; Benning, S. A.; Kitzerow, H.-S.; Achard, M.-F.; Bock, H. *Angew. Chem., Int. Ed.* **2001**, *39*, 2060–2063.
(9) Brabec, C.; Dyakonov, V.; Parisi, J.; Sariciftci, N. S. *Organic Photovotaics*; Springer: Berlin, Germany, 2003.
(10) Carroll, R. L.; Gorman, C. B. *Angew. Chem., Int. Ed.* **2002**, *41*, 4378–4400.
(11) Dimitrakopoulos, C. D.; Malenfant, P. R. L. *Adv. Mater.* **2002**, *14*, 99–117.
(12) Forrest, S. R. *Nature* **2004**, *428*, 911–918.
(13) Chen, J.; Leblanc, V.; Kang, S. H.; Benning, P. J.; Schut, D.; Baldo, M. A.; Schmidt, M. A.; Bulovic, V. *Adv. Funct. Mater.* **2007**, *17*, 2722–2727.
(14) Watson, M. D.; Fechtenkotter, A.; Mullen, K. *Chem. Rev.* **2001**, *101*, 1267–1300.
(15) Tong, Q. X.; Lai, S. L.; Chan, M. Y.; Zhou, Y. C.; Kwong, H. L.; Lee, C. S.; Lee, S. T.; Lee, T. W.; Noh, T. Y.; Kwon, O. Y. *J. Phys. Chem. C* **2009**, *113*, 6227–6230.
(16) Liu, F.; Xie, L. H.; Tang, C.; Liang, J.; Chen, Q. Q.; Peng, B.; Wei, W.; Cao, Y.; Huang, W. *Org. Lett.* **2009**, *11*, 3850–3853.
(17) Liu, W. J.; Zhou, Y.; Zhou, Q. F.; Ma, Y. G.; Pei, J. *Org. Lett.* **2008**, *10*, 2123–2126.
(18) Wu, J. S.; Pisula, W.; Müllen, K. *Chem. Rev.* **2007**, *107*, 718–747.
(19) Moorthy, J. N.; Natarajan, P.; Venkatakrishnan, P.; Huang, D. F.; Chow, T. J. *Org. Lett.* **2007**, *9*, 5215–5218.
(20) Shah, B. K.; Neckers, D. C.; Shi, J. M.; Forsythe, E. W.; Morton, D. *Chem. Mater.* **2006**, *18*, 603–608.
(21) Debad, J. D.; Morris, J. C.; Lynch, V.; Magnus, P.; Bard, A. J. *J. Am. Chem. Soc.* **1996**, *118*, 2374–2379.
(22) Yan, Q.; Zhou, Y.; Ni, B. B.; Ma, Y.; Wang, J.; Pei, J.; Cao, Y. *J. Org. Chem.* **2008**, *73*, 5328–5339.
(23) Chiechi, R. C.; Tseng, R. J.; Marchioni, F.; Yang, Y.; Wudl, F. *Adv. Mater.* **2006**, *18*, 325–328.
(24) Suzuki, K.; Seno, A.; Tanabe, H.; Ueno, K. *Synth. Met.* **2004**, *143*, 89–96.
(25) Tseng, R. J.; Chiechi, R. C.; Wudl, F.; Yang, Y. *Appl. Phys. Lett.* **2006**, *88*, 093512–093514.
(26) Tong, Q. X.; Lai, S. L.; Chan, M. Y.; Zhou, Y. C.; Kwong, H. L.; Lee, C. S.; Lee, S. T. *Chem. Mater.* **2008**, *20*, 6310–6312.
(27) Tong, Q. X.; Lai, S. L.; Chan, M. Y.; Zhou, Y. C.; Kwong, H. L.; Lee, C. S.; Lee, S. T. *Chem. Phys. Lett.* **2008**, *455*, 79–82.
(28) Tong, Q. X.; Lai, S. L.; Chan, M. Y.; Lai, K. H.; Tang, J. X.; Kwong, H. L.; Lee, C. S.; Lee, S. T. *Appl. Phys. Lett.* **2007**, *91*, 153504–153506.
(29) Rosenow, T. C.; Walzer, K.; Leo, K. *J. Appl. Phys.* **2008**, *103*, 043105–043108.
(30) Tirapattur, S.; Belletete, M.; Leclerc, M.; Durocher, G. *J. Mol. Struct.:Theochem* **2003**, *625*, 141–148.
(31) Belletete, M.; Bedard, M.; Leclerc, M.; Durocher, G. *J. Mol. Struct.:Theochem* **2004**, *679*, 9–15.
(32) Arulmozhiraja, S.; Ehara, M.; Nakatsuji, H. *J. Chem. Phys.* **2008**, *129*, 174506–174513.
(33) Pickholz, M.; dos Santos, M. C. *J. Mol. Struct.:THEOCHEM* **2005**, *717*, 99–106.
(34) Ciofini, I.; Laine, P. P.; Bedioui, F.; Adamo, C. *J. Am. Chem. Soc.* **2004**, *126*, 10763–10777.
(35) Jacquemin, D.; Preat, J.; Wathelet, V.; Fontaine, M.; Perpete, E. A. *J. Am. Chem. Soc.* **2004**, *128*, 2072–2083.
(36) Amat, A.; Clementi, C.; De Angelis, F.; Sgamellotti, A.; Fantacci, S. *J. Phys. Chem. A* **2009**, *113*, 15118–15126.
(37) Casida, M. E. In *Recent Advances in Density Functional Methods, Part I*; Chong, D. P., Ed.; World Scientific: Singapore, 1995.
(38) Gross, E. K. U.; Dobson, J. F.; Petersilka, M. In *Density Functional Theory II*; Nalewajski, R. F., Ed.; Springer: Heidelberg. 1996.
(39) Dirac, P. A. M. *Proc. Cambridge Philos. Soc.* **1930**, *26*, 376–385.
(40) Vosko, S. H.; Wilk, L.; Nusair, M. *Can. J. Phys.* **1980**, *58*, 1200–1211.
(41) Becke, A. D. *J. Chem. Phys.* **1993**, *98*, 5648–5652.
(42) Li, W.; Wang, Y.-B.; Pavel, I.; Yuan, Q.; Ye, Y.; Fu, E.-Q.; Luo, M.-D.; Hu, J.-M.; Kiefer, W. *J. Phys. Chem. A* **2005**, *109*, 2878–2886.
(43) Baerends, E. J.; Ricciardi, G.; Rosa, A.; van Gisbergen, S. J. A. *Coord. Chem. Rev.* **2002**, *230*, 5–27.
(44) Zhao, W.; Bian, W. *J. Mol. Struct.:THEOCHEM* **2007**, *818*, 43–49.
(45) Santhanamoorhti, N.; Senthilkumar, K.; Kolandaivel, P. *Mol. Phys.* **2009**, *107*, 1629–1639.
(46) Ren, A. M.; Guo, J. F.; Feng, J. K.; Zou, L. Y.; Li, Z. W.; Goddard, J. D. *Chin. J. Chem.* **2008**, *26*, 55–64.
(47) Di Donato, E.; Vanzo, D.; Semeraro, M.; Credi, A.; Negri, F. *J. Phys. Chem. A* **2009**, *113*, 6504–6510.
(48) Xue, Y. S.; Gong, X. D. *J. Mol. Struct.:THEOCHEM* **2009**, *901*, 226–231.
(49) Xue, Y. S.; Mou, J.; Liu, Y.; Gong, X. D.; Yang, Y. H.; An, L. *Cent Eur. J. Chem.* **2010**, *8*, 928–936.
(50) Parac, M.; Grimme, S. *Chem. Phys.* **2003**, *292*, 11–21.
(51) Zhao, Y.; Truhlar, D. G. *Theor. Chem. Acc.* **2008**, *120*, 215–241.
(52) Jacquemin, D.; Perpete, E. A.; Ciofini, I.; Adamo, C. *J. Chem. Theory. Comput.* **2010**, *6*, 1532–1537.
(53) Dreuw, A.; Head-Gordon, M. *Chem. Rev.* **2005**, *105*, 4009–4037.
(54) Lee, C. T.; Yang, W. T.; Parr, R. G. *Phys. Rev. B* **1988**, *37*, 785–789.
(55) Perdew, J. P.; Burke, K.; Ernzerhof, M. *Phys. Rev. Lett.* **1996**, *77*, 3865–3868.
(56) Perdew, J. P.; Burke, K.; Ernzerhof, M. *Phys. Rev. Lett.* **1997**, *78*, 1396–1396.
(57) Adamo, C.; Barone, V. *J. Chem. Phys.* **1999**, *110*, 6158–6170.
(58) Ernzerhof, M.; Scuseria, G. E. *J. Chem. Phys.* **1999**, *110*, 5029–5036.
(59) Zhao, Y.; Truhlar, D. G. *J. Phys. Chem. A* **2006**, *110*, 13126–13130.
(60) Miertus, S.; Scrocco, E.; Tomasi, J. *J. Chem. Phys.* **1981**, *55*, 117–129.
(61) Fratiloiu, S.; Grozema, F. C.; Koizumi, Y.; Seki, S.; Saeki, A.; Tagawa, S.; Dudek, S. P.; Siebbeles, L. D. A. *J. Phys. Chem. B* **2006**, *110*, 5984–5993.

(62) Degheili, J. A.; Moustafa, R. M.; Patra, D.; Kaafarani, B. R. *J. Phys. Chem. A* **2009**, *113*, 1244–1249.
(63) Frisch, M. J.; Trucos, G. W.; Schlegel, H. B.; Scuseria, G. E.; Robb, M. A.; Cheeseman, J. R.; Scalmani, G.; Barone, V.; Mennucci, B.; Petersson, G. A.; et al. Gaussian 09, Revision A.02, Gaussian, Inc., Wallingford, CT, 2009.
(64) McMasters, D. R.; Wirz, J. *J. Am. Chem. Soc.* **2001**, *123*, 238–246.
(65) Kubo, T.; Shimizu, A.; Sakamoto, M.; Uruichi, M.; Yakushi, K.; Nakano, M.; Shiomi, D.; Sato, K.; Takui, T.; Morita, Y.; et al. *Angew. Chem.* **2005**, *117*, 6722–6726.
(66) Nakano, M.; Takebe, A.; Kishi, R.; Fukui, H.; Minami, T.; Kubota, K.; Takahashi, H.; Kubo, T.; Kamada, K.; Ohta, K.; et al. *Chem. Phys. Lett.* **2008**, *454*, 97–104.
(67) Iketaki, K.; Kanai, K.; Shimizu, A.; Kubo, T.; Wang, Z. H.; Ouchi, Y.; Morita, Y.; Nakasuji, K.; Seki, K. *J. Phys. Chem. C* **2009**, *113*, 1515–1519.
(68) Markovic, S.; Durdevic, J.; Jeremic, S.; Gutman, I. *J. Mol. Model.* **2011**, *17*, 805–810.
(69) Nithya, R.; Santhanamoorhti, N.; Kolandaivel, P.; Senthilkumar, K. *J. Phys. Chem. A* **2011**, *115*, 6594–6602.